International Journal For Advanced Research In Science & Technology
A peer reviewed international journal www.ijarst.in
ISSN: 2457-0362

Based on Genome-Derived Minimal Metabolic Models of MG1655 Escherichia coli, the in-vivo respiratory ATP stoichiometry

M SURESH,Asst.Prof, M.A,B.Ed, moddusuresh55@gmail.com,

J USHA SREE,Asst.Prof, M.A,B.Ed, ushasri115@gmail.com,

G LAXMAN,Asst.Prof, M.A, laxman.g.626@gmail.com,

CH VIJAY KUMAR,Asst.Prof, M.A, vijayprem242@gmail.com,

ABSTRACT:

A genome-scale model of E. coli was used to develop metabolic network models that describe the growth of Escherichia coli on glucose, glycerol, and acetate. The precise stoichiometry of energy producing and consuming processes is one of the metabolic network uncertainties. The ATP stoichiometry is critical to accurate biomass and product yield estimations. Eight distinct aerobic chemostat experiments with E. coli MG1655, cultured at various dilution rates (0.025, 0.05, 0.1, and 0.3 h 1) and on various carbon substrates, were used to determine the unknown ATP stoichiometry parameters of the E. coli network (glucose, glycerol, and acetate). Correct information on biomass composition and precise assessments of net conversion rates under well-defined circumstances are required for proper calculation of the ATP stoichiometry. Based on observations and literature data, a growth rate-dependent biomass composition was developed for this purpose. A metabolic network model was used to estimate an effective P/O ratio of 1.49 0.26 mol of ATP/mol of O, KX (growth-dependent maintenance) of 0.46 0.27 mol of ATP/C-mol of biomass, and mATP (growth independent maintenance) of 0.075 0.015 mol of ATP/C mol of biomass/h after incorporating the growth rate-dependent biomass composition. In order to precisely estimate all other fluxes and yields, just the particular growth rate, m, is required as an input.

KEYWORDS: Energy, P/O ratio, maintenance, and Herbert–Pirt relationships in Escherichia coli

Introduction

Using industrial microbes to make new and better products from renewable resources requires quantitative knowledge of cellular response networks and the management of those networks. This knowledge is critical. An method based on systems biology includes mathematical modeling of metabolism as a key tool. Metabolic engineering of microorganisms is increasingly guided by stoichiometric modeling, which has grown in popularity in the previous decade (Kim et al., 2008). In part, this is due to the fact that stoichiometric modeling only needs to know about the structure of the metabolic network and not about the specific biological events involved. Annotated genome sequences and subsequent curation based on biochemical and physiological information from the associated organism may be used to develop whole genome-scale metabolic networks (Durot et al., 2009). Escherichia coli has had its genome-scale metabolic model extended several times, for example, as work on genomic reconstruction continues (Feist et al., 2007). Realize, however, that the metabolic model does not necessarily need to integrate the whole database of potential reactions for certain well-defined development circumstances. It has been shown that genome-scale reaction datasets may be reduced to specialized metabolic network models by utilizing proper model reduction methods (Burgard et al., 2001). While most metabolic pathways have stoichiometry established, the stoichiometry for some processes remains a mystery, such as the transport mechanisms, compartmentation, and the stoichiometries of the processes themselves, such as the P/O ratio for the generation of ATP and growth-dependent or growth-independent maintenance energy requirements (i.e., KX and mATP). Parameter values are often derived from either theoretical assumptions (Kayser et al., 2005) or in vitro investigations (Varma and Palsson, 1993). (Hempfling and Mainzer, 1975).

ATP stoichiometry parameters may be determined in vivo using Van Gulik and Heijnen (1995)'s new approach. For Saccharomyces cerevisiae and Candida utilis, they used literature data from carbon-limited chemostat cultures at the same growth rate but on different substrates to estimate the P/O ratio and KX. Using just one growth rate for all experiments made it impossible to distinguish between maintenance energy needs that are growth dependent and independent. It was also anticipated that the growth limiting substrate had no effect on the parameters of the experiment. S. cerevisiae growth on glucose and ethanol mixtures, the prediction of operational yields of amino acids, and the derivation of network-derived irreversibility limitations have all been successfully predicted using this technique (Van Gulik and Heijnen, 1995). When it came to the metabolic network in Penicillium chrysogenum, the technique had been expanded to include both growth and

International Journal For Advanced Research In Science & Technology
A peer reviewed international journal www.ijarst.in
ISSN: 2457-0362

penicillin synthesis (Van Gulik et al., 2000). The efficiency of oxidative phosphorylation and the extra amount of ATP dissipation associated with the synthesis of b-lactam molecules were determined from the results of carbon restricted chemostat experiments performed on various substrates and at a variety of different dilution rates. (Van Gulik et al., 2001). Because these stoichiometric models incorporate accurate estimates of the ATP stoichiometry coefficients, they can forecast fluxes for a given substrate and growth and product creation rates, making them very important Such models are also capable of predicting the theoretical maximum biomass and product yields on a given substrate, taking into consideration stoichiometric and thermodynamic limitations. For accurate stoichiometry estimates of metabolic networks, it is critical to provide an accurate biomass composition for each microbe analyzed. In flux-based models, the biomass composition, which is known to be a function of growth rate, must be taken into consideration because of its major impact on flux distribution (Pramanik and Keasling, 1998). According to our research, no prior studies have used in vivo methods to assess the metabolic network models for E. coli ATP stoichiometry in real-world circumstances. For E. coli MG1655 on a chemically defined medium containing glucose, glycerol and acetate as carbon sources, a metabolic network model was developed. Subsets of processes from Reed et al. (2003)'s genome scale model were utilized to create the new models, with the goal of increasing biomass production on substrate. Later, in vivo data were obtained by steady state chemostat cultivations on three distinct substrates at various dilution rates. For a constant biomass composition in relation to growth rate, measurements of the elemental and biochemical content of the biomass were gathered together. ATP stoichiometry parameters were obtained from the chemostat data using a combination of data reconciliation and parameter estimate, which ensured that the elemental conservation relations were fulfilled.

Components and Processes

Stiffness And Growth Factors

The Netherlands Culture Collection of Bacteria provided the strain of E. coli used in this study (NCCB). Luria-Bertani (LB) media was used to grow cells to stationary phase in shake-flasks. Until they were employed as precultures for chemostat studies, culture aliquots containing 50% glycerol were maintained at 808C. 378 C and 220 RPM were used for the growth of precultures on minimum media with the following composition: 1 L. 1 mL of trace element solution (Verduyn et al., 1992) and 40 mM MOPS were used in the preparation of the (NH4)2SO4, 2.0 g KH2PO4, 0.5% MgSO4 in 7H2O, 0.5% NaCl, 2.0 g NH4, and 5.5 g glucose in 1H2O. Pretreatment with 1 M K2HPO4 (FP 30/0.2 CA-S, pore size 0.2 mm, cellulose acetate) resulted in an acidic solution that had to be neutralized before filter sterilization could begin. Chemostat cultures of aerobic organisms with carbon limitations were carried out using minimum media containing three distinct forms of carbon: glucose, glycerol, and ethylacetate. Dilution rates (D) of 0.025, 0.05, 0.1, and 0.3 h 1 were used in the glucose-limited chemostat experiments. The dilution rate used in the acetate and glycerol restricted chemostats was 0.1 h 1. All chemostat tests were performed in fermentors with a working capacity of 4 liters and a volume of 7 liters, all of which were weight-controlled (Applikon, Schiedam, The Netherlands). Except for the carbon source, all chemostat tests used the same minimum medium, which included the following ingredients per liter: 2.0 g NH4Cl, 0.01% thiamine hydrochloride, 2.0 mL of trace elements solution (Verduyn and colleagues, 1992), as well as 0.2 mL of silicone-based antifoaming agent (Verduyn and colleagues, 1992) (BDH, Poole, UK). Glycerol (75.8 mmol/L), acetate (113.6 mmol/L), or glucose (37.9, 75.8, or 151.5 mmol/L) were the carbon sources. The process for preparing the medium and cultivating the plants was the same as previously stated (Taymaz Nikerel et al., 2009). Using an autoclavable dissolved oxygen tension (DOT) sensor (Mettler-Toledo, Greifensee, Switzerland), the culture's DOT was monitored online, although

Table I.

Conditions (substance, concentration of substrate in feed vessel (CS,in), and rate of dilution D) and goal

International Journal For Advanced Research In Science & Technology
A peer reviewed international journal www.ijarst.in
ISSN: 2457-0362

of the chemostat studies.

Chemostat name	Substrate	$C_{S,in}$ (mM)	D (h^{-1})	Purpose
glu1	Glucose	37.9	0.102	P
glu2	Glucose	37.9	0.099	B, P
glu3	Glucose	37.9	0.314	B, P
glu4	Glucose	37.9	0.049	B, P
glu5	Glucose	37.9	0.025	P
gly1	Glycerol	75.8	0.102	P
gly2	Glycerol	75.8	0.099	P
ace1	Acetic acid	113.6	0.097	P
glu6	Glucose	75.8	0.100	B
glu7	Glucose	151.5	0.102	B

Evaluating biomass composition; P, parameter estimates and flux analysis under supervision. No studies were conducted when the DOT fell below 50% air saturation. The batch phase was preceded by chemostat culture on the same medium as the feed medium. It was immediately after the batch phase was completed that medium feeding began, which was indicated by a fast drop in the carbon dioxide evolution rate (CER) and oxygen absorption rate (OUR). This was confirmed by the measured biomass concentration and online measurements of dissolved oxygen and the oxygen and carbon dioxide contents in the offgas after five residence periods in the chemostat.

Procedures for Analyzing Data

Online measurements of CO2 and O2 volume fractions from dry offgas (Perma Pure LLC, Toms River, NJ) were made using a CO2 infrared and an O2 paramagnetic gas analyzer (NGA 2000, Rosemount Analytical, Hasselroth, Germany). Using disposable membrane filters (MILLEX-HV, Millipore, Carrigtwohill Co., Cork Ireland) and quickly collecting broth into syringes containing cold stainless steel beads (208C), we collected broth supernatant samples as described by Mashego et al (2003). Glucose and carbon levels in the broth and the filter were determined as previously reported, as was the case (Taymaz-Nikerel et al., 2009). The quantities of residual glycerol and acetate in the supernatant were determined using an enzymatic kit (R-Biopharm, Boehringer Mannheim, Darmstadt, Germany).

Composition of macromolecules and elements in biomass

E. coli biomass was extracted from steady-state glucose-limited cultures. It was centrifuged for 5 minutes at 48 degrees Celsius (5,000 rpm) and then the cells were rinsed two times with a 0.9% NaCl solution. For 24 hours, the biomass pellet was kept at 808C and then freeze-dried at a pressure of 10 psi for 24 hours (Edwards Modulyo, Sussex, UK). Once frozen, the biomass was kept in a desiccator at room temperature for further investigation. Electronic analyzers assessed the biomass concentrations of carbon (C), hydrogen (H), nitrogen (N), sulfur (S), and oxygen (O) (Elementar, Vario EL III, Hanau, Germany). The Biuret technique was used to determine the total protein content (Herbert et al., 1971)

The Uptake/Sequestration Ratio Must Be Calculated

The mass balances of substrate in the liquid phase and oxygen and carbon dioxide in the gas phase were used to compute the substrate consumption rate (qS), oxygen consumption rate (qO2), and carbon dioxide generation rate (qCO2). Carbon balance for the culture filtrate (qlysis) was computed using the total quantity of carbon generated in the form of dissolved compounds by measuring TOC of the filtrate. We refer to the net conversion rates we arrive at from extrapolating from the raw data as "unbalanced rates."

Ideas and Theories

In E. coli, Oxidative Phosphorylation

Two membrane bound NADH dehydrogenases (NDH1 and NDH2), a quinone pool, and two ubiquinol oxidases (bo-type and bd-type) make up E. coli's aerobic respiratory chain (Calhoun et al., 1993; Neijssel and Teixeira de Mattos, 1994). NDH1 is the homolog of eukaryotic mitochondrial complex I and is thought to have a H/e ratio of 2 among the two NADH dehydrogenases. H/ e 14 0 is not generated by NDH2 in the process of generating the proton motive force (pmf) (Calhoun et al., 1993 and references therein). Bo-type terminal oxidases have a H/e translocation ratio of 2 whereas bd-type terminal oxidases have a H/e translocation ratio of 1. The bd-type terminal oxidases prevail in low oxygen environments, whilst the bo-type terminal oxidases do so in high oxygen environments (Calhoun et al., 1993 and references therein). Succinate dehydrogenase transfers electrons to the quinone pool through FADH2 while operating in aerobic circumstances. Further research suggests that mate dehydrogenase produces pmf across the cell membrane. " According to Ingledew and Poole (1984), the respiratory chain's formate-to-quinone portion transfers two protons. Purine–pyrimidine

International Journal For Advanced Research In Science & Technology
A peer reviewed international journal www.ijarst.in
ISSN: 2457-0362

biosynthesis pathway reaction dihydroorotic acid dehydrogenase contributes electrons to the quinone pool. However, this response has a very little impact. Nearly all of nonlim's components are ubiquinone when exposed to oxygen (Calhoun et al., 1993; Ingledew and Poole, 1984). ubiquinone-8 is essential for the glycerol-3-phosphate dehydrogenase process, which is necessary for the development of organisms on glycerol (Keseler et al., 2009). Oxidative phosphorylation, or the P/O ratio of E. coli in terms of its respiratory chain composition, relies on oxygen availability, as shown in the preceding paragraphs. The theoretical maximal P/O ratio for the ATP synthase is 2 with a H/ATP stoichiometry of 4 (Stahlberg et al., 2001). Table II summarizes the proton translocation stoichiometry for each dehydrogenase in the network.

Stoichiometry of ATP:

An equation for the metabolic network's ATP balance is given by

$$q_{\mathrm{ATP,ox}} - \sum q_i^{\mathrm{ATP}} - K_X\mu - m_{\mathrm{ATP}}=0, \qquad (1)$$

the net rate of ATP consumption in the part of the metabolic network model for which ATP stoichiometry is known, including substrate level phosphorylation, is represented by the first term, and the second term represents oxidative phosphorylation's production of ATP; m is the specific growth rate; KX and mATP represent the growth dependent and growth independent maintenance coefficients, respectively; (Van Gulik et al., 2001). The growth circumstances affect how the respiratory chain's electron flow is distributed among its many components, as described above (e.g., substrate and growth rate). By using PMF generation data for various electron sources (see Table II), it is possible to describe oxidative phosphorylation ATP production as follows:

$$q_{\mathrm{ATP,ox}} = \sum_{i=1}^{n} P/O^i q_{2e}^i \qquad (2)$$

Table II. Stoichiometry of proton translocation and maximum theoretical P/O ratio of each dehydrogenase involved in the *E. coli* metabolic networ

Dehydrogenase		Proton translocation		Max P/O[a]	
NDH1	NADH dehydrogenase	$8H^+/2e^-$	4+4	2	(δ)
NDH2	NADH dehydrogenase	$4H^+/2e^-$	0+4	1	
SUCD4	Succinate dehydrogenase	$4H^+/2e^-$	0+4	1	(α_1)
FDH2	Formate dehydrogenase	$6H^+/2e^-$	2+4	1.5	(α_2)
DHORDT	Dihydroorotic acid dehydrogenase	$4H^+/2e^-$	0+4	1	(α_3)
G3PD5	Glycerol-3-phosphate dehydrogenase	$4H^+/2e^-$	0+4	1	(α_4)

[a]For the calculation of the maximal P/O ratios the H^+/ATP stoichiometry of the ATP synthase was considered to be equal to 4.

For *E. coli* this can be expressed as

$$q_{\mathrm{ATP,ox}} = \delta(q_{\mathrm{NDH}} + \alpha_1 q_{\mathrm{SUCD4}} + \alpha_2 q_{\mathrm{FDH2}} + \alpha_3 q_{\mathrm{DHORD2}} + \alpha_4 q_{\mathrm{G3PD5}}) \qquad (3)$$

A1 through a4 represent the proportionate contributions of the other dehydrogenases to proton translocation, and d represents the NADH P/O ratio. They act together, hence it is impossible to discern a pattern between the two NADH dehydrogenases, NDH1 and NDH2. Only the total flow through the two dehydrogenases is taken into consideration (qNDH). The greatest P/O values for several electron sources are shown in Table II.

$$q_{\mathrm{ATP,ox}} = \delta(q_{\mathrm{NDH}} + 0.5q_{\mathrm{SUCD4}} + 0.75q_{\mathrm{FDH2}} + 0.5q_{\mathrm{DHORD2}} + 0.5q_{\mathrm{G3PD5}}) \qquad (4)$$

Note that qG3PD5 is only significant for growth on glycerol as a source of carbon.

Estimation of Energetic Parameters Using CDR of All Data

In each chemostat experiment, gas and liquid flow rates and the concentrations of chemicals in both phases are measured or set, as well as the experimental errors. Standard data reconciliation procedures uncover the relevant fluxes and covariance matrices for the whole metabolic network given the interaction matrix (van der Heijden et al., 1994; Verheijen, 2010). This equation (Eq. 1) provides a linear equation for each of the chemostat cultivations under varied circumstances (dilution rates and growth-limiting substrates) that have been obtained. After all that work, linear regression provides the most accurate estimations of the energy needs and oxidative phosphorylation efficacy (d) in terms of ATP stoichiometry (d) (Van Gulik et al., 2001).

We've widened the scope of our strategy. When reconciling data from each chemostat experiment, we use Equation (1) as an additional constraint to estimate the fundamental flux balances on each node. For each chemostat experiment, I 14 1,..., n, the weighted sum-of-squares SSid; KX; mATP may be calculated immediately. The overall sum-of-squares is then calculated by adding the sums-of-squares from all of the tests, in this instance n 14 8.

$$\mathrm{SS_T}(\delta, K_X, m_{\mathrm{ATP}}) = \sum_{i=1}^{n} \mathrm{SS}_i(\delta, K_X, m_{\mathrm{ATP}}) \qquad (5)$$

International Journal For Advanced Research In Science & Technology
A peer reviewed international journal www.ijarst.in
ISSN: 2457-0362

The best estimate of these parameters is obtained by minimizing this objective in relation to the three energy parameters, and an estimate of the covariance matrix of the three energy parameters, d, KX, and mATP, is obtained by minimizing the objective's local curvature. Using this method, each experiment is given its own weight and is based on the raw measurements itself. Secondly, we take into account the fact that we use the ATP balance (Eq. 1) in our data reconciliation. As a starting point for the study, this is one of the assumptions we'll use to determine the energy parameters. Because this assumption is supported by results, the inaccuracy in estimated fluxes is lowered as well.

Discussion of the findings

Modeling of a Minimal Metabolic Network Based on the Genome

For the CDR stage, either an objective function (e.g., maximum biomass production on the provided substrate) or reduced reaction sets reflecting determined metabolic sub-models for the multiple substrates are needed. ATP stoichiometry parameters may then be estimated simultaneously. If the same objective function is used to produce the reduced models, both techniques provide the same results. For this project, we've decided to use metabolic models that have been decreased in size. E. coli K12 MG1655's minimum metabolic network was obtained from Reed et al. (2003)'s genome-scale reconstruction of 904 genes and 931 biochemical processes. One reaction is used to represent biomass growth in this reconstruction, with biosynthetic components and ATP being removed from the network as the product. Because the growth rate is known to affect biomass composition, this method does not provide for a simple way to alter this. This necessitated a separate process for the biosynthesis of the primary biomass components (proteins; carbohydrates; lipids; nucleic acids and DNA) and a reaction to synthesize biomass from these constituents.

14 new processes were therefore included to Reed et algenome .'s scale model (2003). In order to establish a minimal reaction set for the description of aerobic glucose-limited growth on a given medium, model reduction was used after the fact. To begin, all 150 transport processes were discarded since the substances they entailed were not present in the growth medium or created by the cells, making them inapplicable under the current cultivation circumstances. There were 264 dead-end reactions that had to be eliminated, therefore the model was reduced to 531 reactions. In the second stage, linear programming was used to determine the flux distribution with the goal of maximizing biomass output on the substrate. 276 non-zero fluxes were found for glucose, which was the only carbon source. After removing the zero flux processes, the metabolic network model for aerobic glucose growth was reduced to its simplest form. In Supplementary Material, you'll find the whole response set. The flux distribution via central metabolism for growth on glucose derived using the reduced model was compared to the reported genome-wide optimum metabolic flux distribution for qS 14 6.6, qO2 14 12:4, and qAcetate 14 1.5 mmol/g/h for glucose growth (Edwards and Palsson, 2000). When it comes to lower glycolysis, TCA cycle, and pentose phosphate pathway flux distribution, this resulted in an almost same flux pattern. In our simplified model (see Biomass Composition Section), we employed a biomass composition somewhat different from that of Edwards and Palsson's (see Biomass Composition Section) (2000). By adding the required catabolic events to the glucose growth model, researchers were able to generate similar models for growth on glycerol and acetate (see Supplementary Material)

Cultivating Chemostats

A minimum of three separate ATP balance equations (Eq. 1) and three independent datasets for qATP,ox, PqATP I and m are needed to estimate the ATP stoichiometry parameters d, KX, and mATP. These may be made by varying the conditions in which E. coli is cultivated in chemostat cultures (substrates and growth rates). The calculated parameters will be more accurate if they are based on more than the bare minimum of three datasets. When it comes to the substrate concentration in the feed medium, all eight chemostat cultivations had the same Cmol/L substrate concentration (227 mCmol/L; see Table I) as a carbon source in the feed medium. A single dilution rate of 0.1 h 1 was used for all of the chemostats, whereas the glucose restricted ones (glu1-glu5) were run at four distinct rates (0.05, 0.1, and 0.31 h 1). The biomass concentration and the oxygen and carbon dioxide concentrations in the offgas were able to demonstrate that the cultures had stabilized after around five residence durations. Remaining substrate concentrations demonstrated that all cultures grew at steady state in a restricted supply of nutrients. For dilution rates ranging from 0.025 to 0.31 h 1, the residual glucose concentrations in the glucose-limited cultures were between 4.5 1.5 and 12.7 1.2 mg/L. 1. Remaining concentrations of glycerol and acetate in the glycerol- and acetate-limited cultures were 2.97 and 0.31 mg/L, respectively. Biomass and substrate conversion rates for all chemostat studies could be calculated using the observed concentration of biomass, substrate, oxygen, and carbon dioxide as

International Journal For Advanced Research In Science & Technology
A peer reviewed international journal www.ijarst.in
ISSN: 2457-0362

well as flow rates of both liquid and gas. In these carbon-limited cultures, HPLC tests verified that the byproducts (acetate, formate, lactate, and succinate) were not formed. However, the TOC level of the culture filtrate indicated that it included a considerable quantity of carbon. Dilution rates below 0.01 h 1 resulted in a filtrate with a total organic carbon (TOC) level that ranged from roughly 16 to 29 mM, respectively, for glucose-limited cultures. Acetate- and glycerol-restricted chemostats had comparable TOC levels to glucose-restricted chemostats (15 and 13 mM, respectively). Growth in glucose-limited chemostats was shown to be glucose-limited even after increasing the glucose concentration in the feed vessel by a factor of four (results not shown). To put it another way, this fourfold increase led to a fourfold rise in the constant biomass concentration and a fourfold rise in the filtrate's total organic carbon content. As previously mentioned, increasing biomass increases the filtrate TOC content.)

Table III. Uptake and secretion rates qi, represented as mmol/CmolX/h per Cmol of biomass (derived from raw measurement data), are unbalanced in steady state aerobic carbon-limited chemostat cultivations of E. coli at various dilution rates with various substrates (mmol/CmolX/h).

Chemostat	D (h^{-1})	C_X (gDW/L)	q_X	$-q_S$	$-q_{O_2}$	q_{CO_2}	q_{Lysis}	Carbon recovery	Redox recovery
glu1	0.102	2.90 ± 0.27	115.2 ± 2.7	30.6 ± 3.1	88.09	81.59	13.0 ± 1.4	107.0	115.3
glu2	0.099	2.63 ± 0.05	113.7 ± 2.3	32.6 ± 1.3	97.09	87.54	14.53 ± 0.59	102.8	112.0
glu3	0.314	2.99 ± 0.22	362.8 ± 8.1	93.6 ± 7.8	211.49	196.41	48.5 ± 4.1	99.5	105.4
glu4	0.049	2.47 ± 0.10	58.8 ± 1.3	16.99 ± 0.90	61.46	51.05	9.38 ± 0.71	107.7	123.3
glu5	0.025	1.96 ± 0.09	33.70 ± 0.78	10.73 ± 0.61	42.63	37.16	8.45 ± 0.54	110.1	123.8
gly1	0.102	2.91 ± 0.06	113.8 ± 2.3	60.3 ± 2.5	98.22	69.53	11.83 ± 0.46	101.4	104.6
gly2	0.099	3.05 ± 0.09	110.2 ± 2.5	56.3 ± 2.6	94.70	65.83	11.1 ± 1.1	104.2	108.1
ace1	0.097	1.44 ± 0.26	117.7 ± 4.5	176 ± 32	229.48	224.29	20.7 ± 3.9	97.2	101.2
glu6	0.100	5.34 ± 0.07	114.1 ± 2.6	32.50 ± 1.2	88.69	87.30	14.0 ± 1.3	103.3	108.4
glu7	0.102	10.24 ± 0.15	119.4 ± 2.6	33.55 ± 1.3	92.94	92.57	17.5 ± 1.3	105.3	109.9

Substrate depletion rate; oxygen consumption rate; carbon dioxide generation rate; biomass lysis; qX, biomass creation rate, are some of the terms used. Percent concentrations of carbon and redox recoveries (as well as lowered dilution rates) strongly imply, as previously reported, that the organic carbon found in the filtrate was the consequence of cell lysis (Taymaz-Nikerel et al., 2009). The presence of cell lysis suggests that the cellular growth rate (m) is not the same as the chemostat's dilution rate, but rather is equal to the dilution rate plus the biomass-specific rate of cell lysis (as shown by the presence of cell lysis) (qlysis). Because growth is a significant ATP drain, failing to account for cell lysis will result in inaccurate flux estimations and, as a result, incorrect estimates of ATP stoichiometry coefficients. The biomass specific conversion rates computed from the primary data as well as the recoveries of carbon and redox are given in Table III. This table shows that the carbon recovery rates were within acceptable ranges. However, severe redox balance aberrations were discovered for several of the glucose-limited chemostats (recoveries up to 123 percent). The oxygen absorption rate is most likely overestimated because of an incorrect measurement of oxygen content in the offgas. For aerobic glucose restricted development, it is predicted that the oxygen intake rate would be somewhat lower than the carbon dioxide generation rate, which was not seen in our chemostat cultures. The ensuing data reconciliation and parameter estimate technique did not employ oxygen readings that were out of whack.

Chemistry of Biomass Elements

C, H, O, N, and S content of freeze-dried biomass samples from the several aerobic glucose-limited cultures were examined. Table IV shows that the elemental compositions in the feed were consistent regardless of the growth rate or the amount of substrate in the feed. It observed that the carbon and nitrogen concentrations were in line with previously reported values for

Table IVE.coli biomass at varied dilution rates (D) and glucose concentrations in the feed (CS,in) with respective standard errors were analyzed.

Chemostat code	D (h^{-1})	$C_{S,in}$ (mM)	C (%)	H (%)	N (%)	O (%)	S (%)
glu4	0.049	37.9	44.36 ± 0.08	7.57 ± 0.03	11.81 ± 0.02	NA	0.41 ± 0.01
glu6	0.100	75.8	43.91 ± 0.05	7.29 ± 0.04	12.25 ± 0.01	28.36 ± 0.29	0.58 ± 0.02
glu2	0.099	37.9	43.46 ± 0.06	7.35 ± 0.05	12.06 ± 0.01	27.66	0.47 ± 0.003
glu2	0.099	37.9	45.09 ± 0.01	7.43 ± 0.03	12.38 ± 0.01	29.17	0.50 ± 0.03
glu7	0.102	151.5	45.47 ± 0.03	7.63 ± 0.02	12.42 ± 0.03	NA	0.47 ± 0.01
glu3	0.314	37.9	43.71 ± 0.03	7.34 ± 0.04	11.93 ± 0.03	NA	0.45 ± 0.02
Average			44.33 ± 0.33	7.44 ± 0.06	12.14 ± 0.10	28.40 ± 0.44	0.48 ± 0.02

On the basis of glucose, aerobic growth (Bratbak and Dundas, 1984; Han et al., 2003; Heldal et al., 1985). It was decided to average the observed elemental compositions for the various growth rates and substrate concentrations in the feed. The average elemental composition came out to be CH2:01N0;23O;48S0:004 (gx 14 4.37). 93% of the biomass is made up of these substances. An ash content is defined as the residual phosphorus and other metal ions. At a dilution rate of 0.09%–0.22%, aerobic glucose-limited E. coli K12 cultures typically produce between 1.93 and 3.00 Cmol biomass/mol glucose, with an average RQ of between 1.03 and 1.11 for dilution rates of 0.09–0.22 h 1. (Emmerling et al., 2002; Fischer and Sauer, 2003; Hua et al., 2003; Johansson et al., 2005; Sauer et al., 1999). According to the RQ

International Journal For Advanced Research In Science & Technology
A peer reviewed international journal www.ijarst.in
ISSN: 2457-0362

study and the range of biomass yields, gx for E. coli is in the range of 4.23–4.41. (see Appendix). In this region, our elementally measured gx of 4.37 falls neatly.

Macromolecular Composition

Despite the lack of published data on E. coli K12 biomass composition cultivated in aerobic carbon-limited chemostat cultures, most writers cite Neidhardt's work (1987). E. coli B/r was grown aerobically at 378C (with a mass doubling time of 40 min) on glucose minimum medium, and the biochemical composition was examined. Dry biomass was found to contain 55% protein, 20.5 percent RNA, 3.1% DNA, 9.1 percent lipids, 3.4% lipopolysaccharides (LPS), 2.5 percent peptidoglycan (PG), 2.5 percent glycogen (14polysaccharide (PS)), 0.4 percent polyamines (0.3 percent putrescine, and 0.1% spermidine), and 3.5% other metabolites, cofactors, and ions, with a calculated elemental Some macromolecules have been quantified in earlier research, but the composition provided by Neidhardt (1987) was utilized for the unmeasured molecules. Environmental factors and growth rate are known to alter the biomass's macromolecular composition (Bremer and Dennis, 1996). However, the protein content of E. coli cells grown in glucose-limited chemostats did not vary appreciably with changes in specific growth rate, as measured by our measurements of protein content. Measured protein content closely correlated with previously reported values (Table V). Table V (Emmerling et al., 2002) data, which show a linear relationship between RNA content and specific growth rate, was employed since the RNA measurements were not repeatable.

Calculate the RNA content as a function of the growth rate of the organism. The RNA/DNA ratio was used to assess the DNA content (Neidhardt, 1987). Pramanik and Keasling determined the composition of amino acids in an aerobic chemostat under glucose limitation (1998). For E. coli proteins, differences across strains and/or growing conditions were found to be minor. Because the protein's amino acid content doesn't alter with growth rate, the ribonucleotide composition of RNA shouldn't fluctuate much (Pramanik and Keasling, 1998). Deoxyribonucleo tides in DNA should not be affected by growth rate, but the overall DNA content would (Pramanik and Keasling, 1998). An exact ratio was allocated to each of the remaining organic biomass components: lipids; LPS; PS; PG; putrecine; and spermidine (Neidhardt, 1987). In the elemental analysis portion, the ash content was also considered to be growth rate independent. The average elemental composition was determined to be CH1:63N0:25 O0:38S0:006, with a generalized degree of reduction gx 14 4.18. There was a noticeable difference between the predicted elemental composition and the average measured elemental composition, which was computed from Table IV as CH2:01N0:23O0:48S0:004. According to Table IV, the difference between the elemental and biochemical compositions of the biomass suggests that the biomass has been reduced significantly. Elements (as a percentage of dry weight) in the E. coli biomass were analyzed to determine their standard errors at various dilution rates (D) and glucose concentrations in the feed .

Table V. Protein and RNA concentrations in E. coli grown in aerobic glucose-limited chemostat cultures have been reported in the literature (as a percentage of dry weight).

E. coli strain	D (h^{-1})	Protein (%)	RNA (%)	References
JM101	0.09	69.8	7.2	Emmerling et al. (2002)
JM101	0.4	61.7	15.4	Emmerling et al. (2002)
K12 W3110	0.1	70	7	Hua et al. (2003)
K12 MG1655	0.12	70.1	4.7	Fischer and Sauer (2003)

implying that the latter is incorrect Only lipids have a decrease rate greater than 4.2 when expressed as a percentage of total biomass (in Cmol). If this is correct, the cellular lipid content must have been greater than the 9.1 percent that Neidhardt observed in cells growing at a considerably faster pace (1.0 h 1) than we used in our chemostats (between 0.03 and 0.4 h 1). Microbes with slower growth rates, such as Bacillus megaterium (Sud and Schaechter, 1964) and E. coli (Ballesta and Schaechter, 1972) and Streptococcus faecium (Ballesta and Schaechter, 1972), have higher total lipid contents (Carson et al., 1979). The observed average elemental composition yielded a reduction degree of 4.37, which corresponds to a biomass lipid content of 14.5%. After increasing the lipid content, the elemental composition derived from the biochemical composition was compared to the measured one and found that hydrogen and oxygen concentration differed. The freeze dried biomass may still include some residual water, which is most likely to blame. Yeast samples have already shown this behaviour (Lange and Heijnen, 2001). Macromolecular and elemental compositions of biomass were determined for particular growth rates between 0.025% and 0.3%, as shown in Table VI. The minimum metabolic network models mentioned above were then employed in the data

International Journal For Advanced Research In Science & Technology
A peer reviewed international journal
www.ijarst.in
ISSN: 2457-0362

reconciliation and parameter estimation phase. Note that Neidhardt's biomass composition yields a gx of 4.12, which is within the observed pattern of decreasing gx with increasing growth rate (see Table VI). A high growth rate (late exponential phase) in harvesting the biomass is not unusual in this case.

Reconciling Data and Estimating Energetic Parameters in Real Time Data Reconciliation and Energetic Parameter Estimation in the Same Step

Simultaneous data reconciliation and parameter estimation were performed using data from eight steady-state carbon-limited chemostat cultures at different dilution rates on three different substrates (glucose, glycerol and acetate; see Table I) whose carbon supply in the feed was the same (227 mCmol/L). We used the CDR process outlined in the materials and methods section to reconcile all eight sets of primary data (measured concentrations, flow rates, and volumes). Under the constraint of satisfying the elemental conservation rules, this technique produces the best estimates of the main measurements and net conversion rates (i.e., balanced conversion rates), as well as the best estimates of the three ATP stoichiometry parameters d, KX, and mATP. Additional parameter estimates have been carried out to see whether the pace of growth and the carbon source have a substantial impact on the values of these parameters. While we allowed for various values for the four growth rates, KX and mATP were regarded as single universal factors, as they had been in previous experiments. All three ATP parameters, as well as growth rate and carbon source, were recalculated. The simplified model with three independent universal ATP parameters was shown to be the most accurate in all six scenarios.

Table VI. Composition of the E. coli macromolecular biomass when cultivated in an aerobic glucose-limited culture.

	$D=0.025\,h^{-1}$	$D=0.05\,h^{-1}$	$D=0.1\,h^{-1}$	$D=0.3\,h^{-1}$
Protein	63.95	64.81	68.19	65.43
RNA	5.21	5.86	7.26	13.06
DNA	0.79	0.89	1.10	1.98
Total lipids	20.18	18.80	14.54	11.20
glyc	6.30	5.87	4.54	3.49
etha	3.79	3.53	2.73	2.11
hdca	4.34	4.04	3.12	2.41
hdcea	3.33	3.10	2.40	1.85
ocdcea	2.42	2.26	1.74	1.34
Lipopolysaccharides	1.18	1.10	0.85	0.65
Polysaccharide = glycogen	0.87	0.81	0.62	0.48
Peptidoglycan = murein	0.87	0.81	0.62	0.48
Putrescine	0.40	0.37	0.29	0.22
Spermidine	0.13	0.12	0.10	0.07
Ash	6.43	6.43	6.43	6.43
Sum	100.00	100.00	100.00	100.00
Biomass composition	$CH_{1.74}N_{0.24}O_{0.35}S_{0.004}P_{0.005}$	$CH_{1.72}N_{0.24}O_{0.35}S_{0.004}P_{0.005}$	$CH_{1.69}N_{0.25}O_{0.35}S_{0.007}P_{0.007}$	$CH_{1.64}N_{0.27}O_{0.37}S_{0.007}P_{0.012}$
γ_x	4.41	4.38	4.31	4.21

The percentage of cell dry weight that each macromolecule accounts for is listed. Protein content was determined. The information in Table V was used to make an educated guess about the RNA concentration. The RNA/DNA ratio, reported by Neidhardt, was used to measure the DNA concentration (1987). Glycerol, ethanolamine, hdca, C16:0 fatty acid, hdcea, C16:1 fatty acid, and ocdcea, C18:1 fatty acid are all lipid components. a constant ash content of 6.43 percent was predicted to remain constant throughout time

Table VII. Uptake and secretion rates, qi, of E. coli grown in carbon-limited chemostats at various dilution rates, represented as mmol/CmolX/h per Cmol of biomass (reconciled).

Chemostat	q_X	$-q_S$	$-qO_2$	qCO_2	q_{lysis}
glu1	116.0±2.7	33.3±0.7	74.7±1.2	83.6±1.5	13.9±0.8
glu2	113.0±2.5	32.51±0.65	73.4±1.2	82.0±1.4	14.22±0.51
glu3	365.1±8.5	95.9±2.1	192±4	210±4	50.6±2.1
glu4	59.0±1.4	18.82±0.37	48.3±0.7	53.9±0.8	9.8±0.7
glu5	34.5±0.9	12.52±0.22	37.1±0.4	40.6±0.5	9.29±0.47
gly1	113.7±2.5	61.2±1.2	91.6±1.5	69.8±1.1	11.89±0.36
gly2	110.2±2.7	59.5±1.3	89.5±1.6	68.2±1.2	11.3±1.1
ace1	116.3±2.9	162±4	199±4	208±4	19.2±1.2

Substrate depletion rate; oxygen consumption rate; carbon dioxide generation rate; biomass lysis; qX, biomass creation rate, are some of the terms used.

Growth rate and carbon source could not be rejected with a P-value of 58 percent or higher in the corresponding F-test. Consequently, the ATP stoichiometry parameters were regarded as independent of the growth rate and the substrate employed. Table VII shows the particular net conversion rates m, qS, qO2, etc. that were achieved in the balanced biomass. Analysis of rates

International Journal For Advanced Research In Science & Technology
A peer reviewed international journal www.ijarst.in
ISSN: 2457-0362

and/or system definitions showed no evidence of substantial mistakes based on the statistical criteria (chi square test with the null hypothesis of significant measurement deviations at a significance level 0.1 percent) employed. Table VIII shows the ATP stoichiometry estimates. This table shows that the calculated d is far lower than the theoretical maximum (2.0). No matter how much oxygen is present (as in our chemostat cultures), both the bo-type terminal oxidase and the NDH2 dehydrogenase, which is not involved in PMF production, may be found in large concentrations (see Theoretical Aspects Section). A value of between 1.0 and 2.0 is predicted under these circumstances, which is close to the projected value of 1.49.

Attempting to compare in vivo P/O findings with published values for E. coli is pointless as P/O was always theoretically assumed or obtained from in vitro investigations, as described earlier on in the introductory section. Assuming comparable error estimates, the mATP value of 0.075 0.015 mol/Cmol/h (14 3.2 0.7 mmol/ g/h) calculated here compares well with previous estimates of 2.81 mmol/g/h (Kayser et al., 2005) and 2.81 mmol/g/h (Farmer and Jones, 1976). It was calculated that the growth independent (mATP) and growth dependent maintenance parameters of E. coli K12 MG1655 were 8.4 and 59.8 millimoles per kilogram of dry weight per hour. Both findings are much higher than our projections for growth independent and dependent maintenance parameters of 3.2 0.7 mmol/g/h and 19.8 12 mmol/g, respectively, of these values. Because Feist et al. (2007) relied on previously published chemostat data from many distinct E. coli strains grown on a variety of basic media, these discrepancies might be the result of the authors using a P/O ratio that was much greater than what we anticipated. They did not specify whatever value of the P/O ratio they utilized for their calculations, which is a pity. The comparison of our E. coli findings with those for S. cerevisiae (Van Gulik and Heijnen, 1995) and P. chrysogenum (Van Gulik et al., 2001) is also relevant (Table VIII). E. coli's d is estimated to be in the middle of that of S.

cerevisiae and P. chrysogenum. When compared to P. chrysogenum, the growth-related maintenance coefficient for E. coli was the same, while the growth-independent maintenance coefficient was two times greater. An operational biomass yield on substrate may be calculated using the metabolic network model and the predicted energy parameters. Figure 1 shows operational biomass yields on substrate based on calculated and observed values. This graph shows that the experimental biomass yields on substrate are quite near to the predicted values for all of the varied growth conditions that were used in the experiment. Using this data, we may be certain that our assumption that these ATP coefficients are independent of growth rate and substrate is correct.

Table VIII. Standard errors and comparison with previously reported values for S. cerevisiae and P. chrysogenum (Van Gulik and Heijnen, 1995) ATP stoichiometry parameters for the bacterial metabolic network in E. coli (Van Gulik et al., 2001). Analysis of published parameters for S. cerevisiae (Van Gulik and Heijnen 1995) and P. chrysogenum ATP stoichiometry for E. coli metabolic network (Van Gulik et al., 2001).

	$\frac{1}{\beta}$ (mol ATP/½ mol O_2)	K_X (mol ATP/CmolX)	m_{ATP} (mol ATP/CmolX/h)
E. coli	1.49 ± 0.26	0.46 ± 0.27	0.075 ± 0.015
S. cerevisiae[a]	1.20	0.80	–
P. chrysogenum[b]	1.84 ± 0.08	0.38 ± 0.11	0.033 ± 0.012

The protein concentration was set at 50% with a MW of 26.4 g/Cmol to express KX per Cmol of biomass; however, mATP was not measured. b The 95 percent confidence ranges for errors were provided.

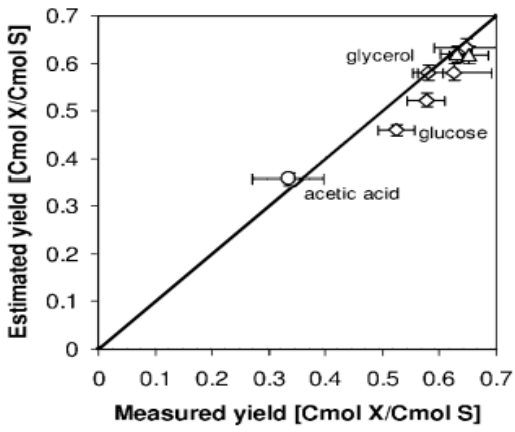

Figure 1. The best estimations of the ATP-stoichiometry parameters were used to compare observed biomass yields on substrate with predicted yields (diamonds: glucose-limited, triangles: glycerol-limited, and circle: acetate-limited).

Analysis of Flux

CDR method was used to concurrently estimate the fluxes across E. coli's metabolic network for growth on glycerol, acetate, and glucose while calculating the parameter values of d, KX, and mATP (see Supplementary Material for fluxes). Using a 0.1 h 1 dilution rate, Figure 2 depicts the

International Journal For Advanced Research In Science & Technology
A peer reviewed international journal www.ijarst.in
ISSN: 2457-0362

flux distribution via central carbon metabolism, with a biomass production rate qX of around 110 mCmol/CmolX/h, which equates to a specific growth rate m = 0.115h 1. In the literature, the G6P node split ratio between glycolysis and PPP under glucose-limited circumstances is often inconsistent. A range of 28 percent to 72 percent (Chassagnole et al., 2002; Schmid et al., 2004) was recorded for this ratio at D 14 0.1 h 1. (Schmid et al., 2004). Fig. 2 shows that our results are in good agreement with the ratio of 56%/44% determined by (Schaub et al., 2008) with ID-13C MFA in wild-type E. coli W3110 at D 14 0.09 h 1, and with the ratio of 54%/44% determined by (Emmerling et al., 2002) with NMR based IS-13C MFA in wild-type E. coli JM101 at D 14 0.09 h 1... Previously, similar split ratios between glycolysis and PPP were observed: 53%/46% (Schmidt et al., 1999), 57%/41% for E. coli K12 at D 14 0.066 h 1 (Kayser et al., 2005), and 63%/34% for E. coli K12 at D 14 0.10 h 1 (Kayser et al., 2005), respectively (Siddiquee et al., 2004). When acetate is the only carbon source, isocitrate dehydrogenase (ICDH) and isocitrate lyase serve as a crucial branch point (ICL). In our results, the distribution of ICDH/ICL is 55%/20% when fluxes are reported on a molar basis and adjusted to the acetate absorption rate (Fig. 2). This is in line with the previously reported values of 53% / 21% at D 14 0.11 h 1 for E. coli K12 (Zhao and Shimizu, 2003). According to Pramanik and Keasling (1997), 71%/13% of the flow was toward a-ketoglutarate rather than glyoxylate, which may be owing to a misinterpretation of how NADH and NADPH interact in the isocitrate dehydrogenase process. When glycerol is restricted, fructose biphosphatase (FBP) flow is equivalent to 13% of the glycerol consumption rate under these circumstances (Fig. 2). 80 percent of glycerol consumption occurs through 13dPG, which is quite close to the 81 percent reported by Holms (1996) for E. coli ML308 cultivated in batch culture at the junction of G3P.

Relationships between Herbert and Pirt

Substrate consumption is described by the Herbert–Pirt equation as a linear link between the growth rate m and the product generation rate qP. (if any). Black box model that depicts how consumed substrate is allocated among growth, maintenance, and product production under varied circumstances may be studied (growth and product formation rates). The parameters of these relationships are the maximum biomass and product yield coefficients on substrate and the maintenance coefficient.. The rate of oxygen consumption and the rate of carbon dioxide generation have similar relationships that may be deduced. A metabolic model may be used to generate these linear relationships (Van Gulik et al., 2001). As shown in Table IX, the Herbert–Pirt equations for substrate, oxygen, and carbon dioxide are calculated for each of the three distinct carbon sources studied. The inverse of the coefficient of m is the maximum yield. There were maximum biomass outputs of 0.66 Cmol X/C Mol glucose, 0.70 Cmol X/C Mol Glycerol, and 0.39 Cmol X/C Mol Acetate on the substrates examined. Glycerol, glycerol and acetate yielded 2.27, 1.71, 0.69 Cmol X/O2 and 1.93, 2.36 and 0.65 Cmol X/CO2, respectively, at their maximum yields.

Conclusions

Minimum metabolic network models may be created for development on a minimal medium under well-defined circumstances from a big genome-scale model, according to this study. In order to explore the stoichiometry of E. coli K12 for three substrates (glucose, glycerol, and acetate) in aerobic substrate restricted chemostats at varying dilution rates, the simplest models produced were employed. Chemostat cultivations had substantial cell lysis (10–25%), which was accounted for in the flow estimates.. Chemostat cultivations were used. Biomass composition was also integrated into the metabolic networks, where protein content was evaluated and the relationship between RNA and DNA and growth rate was determined from literature data. The lipid and carbohydrate contents of biomass were also taken into consideration.

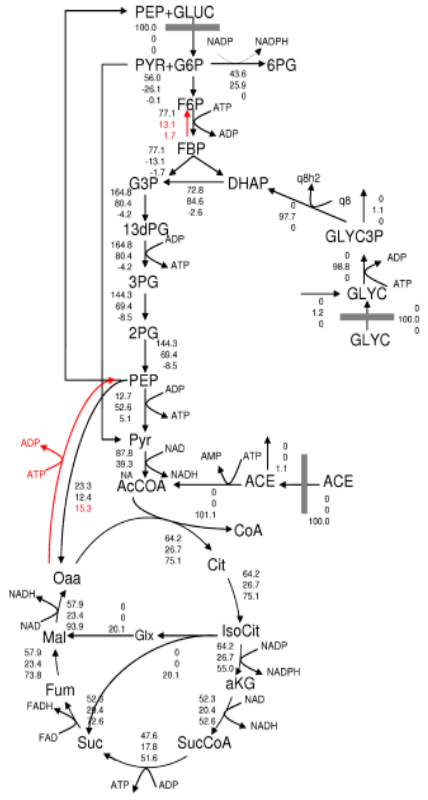

International Journal For Advanced Research In Science & Technology
A peer reviewed international journal www.ijarst.in
ISSN: 2457-0362

Figure 2. Anaerobic growth of Escherichia coli on glucose, glycerol, and acetate was used to calculate central carbon metabolism flow patterns at a dilution rate of 0.01 h 1. All fluxes are shown as a percentage of substrate uptake rate. Glycerol and acetate growth are represented by the first two figures, while glucose growth is represented by the third. Comparing the responses shown with red arrows to growth on glucose, they are the opposite of what they should be.

Table IX. Based on the E. coli metabolic networks developed for each substrate (all rates are reported in mol/CmolX/h), Herbert–Pirt relationships are generated.

Substrate	Herbert-Pirt relations		
Glucose	$-q_S = 0.25\mu + 0.0036$	$-q_{O_2} = 0.44\mu + 0.022$	$q_{CO_2} = 0.52\mu + 0.022$
Glycerol	$-q_S = 0.47\mu + 0.0066$	$-q_{O_2} = 0.58\mu + 0.023$	$q_{CO_2} = 0.42\mu + 0.020$
Acetate	$-q_S = 1.27\mu + 0.018$	$-q_{O_2} = 1.46\mu + 0.023$	$q_{CO_2} = 1.54\mu + 0.036$

Measured elemental composition was used to estimate biomass. E. coli K12 metabolic network for aerobic carbon constrained growth may be estimated simultaneously using the CDR approach, which is based on an accurate growth rate and biomass compositions. To compare with other animals' measurements, we found that our in-vivo estimates of d, KX and mATP had great fit and accuracy. It seemed reasonable to assume that the particular growth rate and substrate were unrelated characteristics. Using simply m as an input, the network model was able to calculate all fluxes. Using labeled C assays, we were able to derive flux pattern/split ratios for the three substrates that were in excellent agreement with previously published data. As a result of the Herbert–Pirt relations, the metabolic network model can calculate the maximum biomass yields on substrate. To thank Gert van der Steen for the elemental analysis of biomass, the authors express their gratitude. The Institute for the Promotion of Innovation through Science and Technology in Flanders provided financial assistance for this study as part of the IWT-SBO project MEMORE (040125). (IWT Vlaanderen). As part of the Netherlands Genomics Initiative/Netherlands Organization for Scientific Research's research agenda, the Kluyver Centre for Genomics of Industrial Fermentation conducted this study.

Relationship between biomass composition and RQ for cultures that use glucose as substrate in the Appendix

When no products are formed, the carbon balance is expressed as follows:

$$q_{CO_2} + \mu = 6q_S \qquad (6)$$

as well as the broad balance of decrease

$$24q_S - 4q_{O_2} = \gamma_x \mu \qquad (7)$$

To calculate the respiratory quotient (RQ), the formula is: qCO2=qO2. Y 14 m=qS results when this information is combined with the measured biomass yield.

$$\gamma_x = \frac{4}{Y}\left[6 - \frac{6 - Y}{RQ}\right] \qquad (8)$$

Equation (8) demonstrates the link between yield of biomass on substrate (Y), degree of reduction of biomass (gx) and RQ. This suggests that under the circumstances of no byproduct production, the existing measurements of offgas and measurement of biomass output would provide the degree of decrease of biomass generated. As an example, putting in a typical yield of 3 Cmol X/mol glucose, and RQ ¼ 1.05 (Sauer et al., 1999) for aerobic glucose-limited chemostat cultures of E. coli, produces gx¼ 4.2.

References

[1] Ballesta JP, Schaechter M. 1972. Dependence of the rate of synthesis of phosphatidylethanolamine and phosphatidylglycerol on the rate of growth of Escherichia coli. J Bacteriol 110(1):452–453.

[2] Bratbak G, Dundas I. 1984. Bacterial dry matter content and biomass estimations. Appl Environ Microbiol 48(4):755–757.

[3] Bremer H, Dennis PP. 1996. Modulation of chemical composition and other parameters of the cell by growth rate. In: Neidhardt FC, Curtiss R, Ingraham JL, Lin ECC, Low KB, Magasanik B, Reznikoff WS, Riley M, Schaechter M, Umbarger HE, editors. Escherichia coli and Salmonella. Cellular and molecular biology. Washington, DC: American Society for Microbiology. p. 1527–1542.

[4] Burgard AP, Vaidyaraman S, Maranas CD. 2001. Minimal reaction sets for Escherichia coli metabolism under different growth requirements and uptake environments. BiotechnolProgr 17(5):791–797.

[5] Calhoun MW, Oden KL, Gennis RB, de Mattos MJ, Neijssel OM. 1993. Energetic efficiency of

Escherichia coli: Effects of mutations in components of the aerobic respiratory chain. J Bacteriol 175(10):3020–3025.

[6] Carson D, Pieringer RA, Daneo-Moore L. 1979. Effect of growth rate on lipid and [7] [7] lipoteichoic acid composition in Streptococcus faecium. BiochimBiophys Acta 575(2):225–233.

[7] Chassagnole C, Noisommit-Rizzi N, Schmid JW, Mauch K, Reuss M. 2002. Dynamic modeling of the central carbon metabolism of Escherichia coli. BiotechnolBioeng 79(1):53–73.

[8] Durot M, Bourguignon PY, Schachter V. 2009. Genome-scale models of bacterial metabolism: Reconstruction and applications. FEMS Microbiol Rev 33(1):164–190.

[9] Edwards JS, Palsson BO. 2000. The Escherichia coli MG1655 in silico metabolic genotype: Its definition, characteristics, and capabilities. Proc Natl Acad Sci USA 97(10):5528–5533.

[10] Emmerling M, Dauner M, Ponti A, Fiaux J, Hochuli M, Szyperski T, Wu¨thrich K, Bailey JE, Sauer U. 2002. Metabolic flux responses to pyruvate kinase knockout in Escherichia coli. J Bacteriol 184(1):152– 164.

[11] Farmer IS, Jones CW. 1976. The energetics of Escherichia coli during aerobic growth in continuous culture. Eur J Biochem 67(1):115–122.

[12] Feist AM, Henry CS, Reed JL, Krummenacker M, Joyce AR, Karp PD, Broadbelt LJ, Hatzimanikatis V, Palsson BO. 2007. A genome-scale metabolic reconstruction for Escherichia coli K-12 MG1655 that accounts for 1260 ORFs and thermodynamic information. Mol SystBiol 3:121.

[13] Fischer E, Sauer U. 2003. A novel metabolic cycle catalyzes glucose oxidation and anaplerosis in hungry Escherichia coli. J Biol Chem 278(47): 46446–46451.

[14] Han L, Enfors SO, Haggstrom L. 2003. Escherichia coli high-cell-density culture: Carbon mass balances and release of outer membrane components. Bioprocess Biosyst Eng 25(4):205–212. Table IX.

[15] Herbert–Pirt relations derived from the constructed E. coli metabolic networks for each substrate (all rates are expressed in mol/CmolX/h).

[16] BiotechnolBioeng 60(2):230–238. Reed JL, Vo TD, Schilling CH, Palsson B. 2003.

[17] An expanded genome-scale model of Escherichia coli K-12. Genome Biol4:R54. Sauer U, Lasko DR, Fiaux J, Hochuli M, Glaser R, Szyperski T, Wuthrich K, Bailey JE. 1999.

[18] Metabolic flux ratio analysis of genetic and environmental modulations of Escherichia coli central carbon metabolism. J Bacteriol 181(21):6679–6688. Schaub J, Mauch K, Reuss M. 2008.

[19] Metabolic flux analysis in Escherichia coli by integrating isotopic dynamic and isotopic stationary 13C labeling data. BiotechnolBioeng 99(5):1170–1185.

[20] Schmid JW, Mauch K, Reuss M, Gilles ED, Kremling A. 2004. Metabolic design based on a coupled gene expression-metabolic network model of tryptophan production in Escherichia coli. Metab Eng 6(4):364– 377.

[21] Schmidt K, Nielsen J, Villadsen J. 1999. Quantitative analysis of metabolic fluxes in Escherichia coli, using two-dimensional NMR spectroscopy and complete isotopomer models.

[22] J Biotechnol 71(1–3):175–189. Siddiquee KAZ, Arauzo-Bravo MJ, Shimizu K. 2004. Metabolic flux analysis of pykF gene knockout Escherichia coli based on 13C-labeling experiments together with measurements of enzyme activities and intracellular metabolite concentrations.

[23] Appl MicrobiolBiotechnol 63(4):407– 417. Stahlberg H, Muller DJ, Suda K, Fotiadis D, Engel A, Meier T, Matthey U, Dimroth P. 2001. Bacterial Naþ-ATP synthase has an undecameric rotor. EMBO Rep 2(3):229–233. Stouthamer A. 1973.

[24] A theoretical study on the amount of ATP required for synthesis of microbial cell material. Antonie van Leeuwenhoek 39(3): 545–565. Sud IJ, Schaechter M. 1964. Dependence of the content of cell envelopes on the growth rate of Bacillus megaterium. J Bacteriol 88:1612–1617. Taymaz-Nikerel H, de Mey M, Ras C, ten Pierick A, Seifar RM,

[25] van Dam JC, Heijnen JJ, van Gulik WM. 2009. Development and application of a differential method for reliable metabolome analysis in Escherichia coli. Anal Biochem 386(1):9–19.

[26] van der Heijden RTJM, Heijnen JJ, Hellinga C, Romein B, Luyben KCAM. 1994. Linear constraint relations in biochemical reaction systems. I. Classification of the calculability and the balanceability of conversion rates. BiotechnolBioeng 43(1):3–10.

[27] Van Gulik WM, Heijnen JJ. 1995. A metabolic network stoichiometry analysis of microbial growth and product formation. BiotechnolBioeng 48(6):681–698.

[28] Van Gulik WM, de Laat WTAM, Vinke JL, Heijnen JJ. 2000. Application of metabolic flux analysis for the identification of metabolic bottlenecks in the biosynthesis of penicillin-G. BiotechnolBioeng 68(6):602–618.

[29] Van Gulik WM, Antoniewicz MR, deLaat WTAM, L VJ, Heijnen JJ. 2001. Energetics of growth and penicillin production in a high-producing strain of Penicillium chrysogenum. BiotechnolBioeng 72(2):185–193.

[30] Varma A, Palsson BO. 1993. Metabolic capabilities of Escherichia coli. II. Optimal growth patterns. J Theor Biol 165(4):503–522. Verduyn C, Postma E, Scheffers WA,

[31] van Dijken JP. 1992. Effect of benzoic acid on metabolic fluxes in yeasts: A continuous-culture study on the regulation of respiration and alcoholic fermentation. Yeast 8(7):501– 517.

[32] Verheijen PJT. 2010. Data reconciliation and error detection. In: Smolke CD, editor. The metabolic pathway engineering handbook. Fundamentals. Boca Raton, FL: CRC Press. Zhao J, Shimizu K. 2003.

[33] Metabolic flux analysis of Escherichia coli K12 grown on 13C-labeled acetate and glucose using GC-MS and powerful flux calculation method. J Biotechnol 101(2):101–117.